Applied Nanoscience
https://doi.org/10.1007/s13204-023-02877-4

ORIGINAL ARTICLE

Theoretical modeling of magnetic field effects on the optical properties of type-II core–shell quantum dot

Volodymyr Holovatsky[1] · Ihor Holovatskyi[2] · Marina Chubrei[2] · Carlos A. Duque[3]

Received: 12 December 2022 / Accepted: 13 May 2023
© King Abdulaziz City for Science and Technology 2023

Abstract

This study presents a simple model within the effective mass approximation to describe the magnetic field impact on the energy structure and interband optical quantum transitions in type-II ZnTe/CdSe and CdSe/ZnTe spherical quantum dots. The dependencies energy spectra and wave functions of an electron and hole on the magnetic field are calculated by the diagonalization method for spherical quantum dots of different sizes. It is shown that the magnetic field violates the spherical symmetry of the system and takes off the degeneration of the energy spectrum concerning the magnetic quantum number. For QD ZnTe/CdSe, the energy of the electron, and for QD CdSe/ZnTe, the energy of the hole in the states with $m \geq 0$ increases when the magnetic field enhances; for the states with $m < 0$, these dependences are non-monotonous (decreasing at first and then increasing). Moreover, the ground state of an electron for QD ZnTe/CdSe and the ground state of a hole for QD CdSe/ZnTe are formed alternately by the lowest states $m = 0, -1, -2, \ldots$ with increasing the induction of magnetic field (Aharonov–Bohm effect). The dependencies of the oscillator strength and the quantum energy transition on magnetic field induction are calculated.

Keywords Core–shell quantum dot · Type-II band alignment · Quasiparticle energy spectrum · Quasiparticle wave function · Oscillator strength · Quantum transition · Magnetic field

Introduction

Semiconductor multilayer quantum dots represent a promising class of nanostructures that can provide new methods of influencing the energy spectrum and wave functions of quasiparticles to obtain the desired optical properties of nanosystems. As a result of the different spatial localization of quasiparticles in multilayer quantum dots, the energy spectrum of electrons and holes can be individually adjusted, which allows to achieve multi-colored radiation with the required spectrum. Therefore, multilayer spherical QDs are intensively studied in both theoretically and experimentally (Nizamoglu and Demir 2008; Nizamoglu et al. 2008; Zhang et al. 2009; Kim et al. 2012; Tyagi and Kambhampati 2012).

The simplest multilayered spherical quantum dots are colloidal core/shell nanocrystals, which contain at least two semiconductor materials in an onionlike structure. The ability to improve the basic optical properties of nanocrystals, such as quantum yield and lifetime, by growing an epitaxial shell from another semiconductor has contributed to significant progress in the chemical synthesis of these nanostructures.

Ihor Holovatskyi, Marina Chubrei, and Carlos A. Duque contributed equally to this work.

✉ Volodymyr Holovatsky
v.holovatsky@chnu.edu.ua

Ihor Holovatskyi
holovatskyi.ihor@chnu.edu.ua

Marina Chubrei
chubrei.maryna@chnu.edu.ua

Carlos A. Duque
cduque_echeverri@yahoo.es

[1] Department of Thermoelectricity and Medical Physics, Chernivtsi National University after Yuriy Fed'kovych, Kotsiubynsky str, 2, Chernivtsi 58002, Ukraine

[2] Department of Information Technologies and Computer Physics, Chernivtsi National University after Yuriy Fed'kovych, Kotsiubynsky str, 2, Chernivtsi 58002, Ukraine

[3] Grupo de Materia Condensada-UdeA, Instituto de Física, Facultad de Ciencias Exactas y Naturales, Universidad de Antioquia UdeA, Calle 70 No. 52-21, Medellín, Colombia

Published online: 30 May 2023

Depending on the band alignment, core–shell QDs are divided into type-I and type-II. In type-I core–shell QDs, the outer shell forms a the potential barrier for quasiparticles and thereby separates the optically active core from the environment, thus increasing the radiation efficiency (Reiss et al. 2009; Wang et al. 2018; AbouElhamd et al. 2019).

In type-II systems, the spatial separation of quasiparticles in different potential wells leads to a smaller effective bandgap than that of each of the constituent materials of the core and shell, resulting in a significant red shift of the emission wavelength. Such features of type-II QDs are proposed to be used in a wide variety of applications, such as light-emitting diodes, detectors, fluorescent labels, and photovoltaics (Jiao et al. 2015; Ma et al. 2013; Long et al. 2019; Verma et al. 2013; Selopal et al. 2020).

Essential for use in solar cells is the rapid separation of charges formed by the photon absorption at the core–shell interface of type-II QDs, where the wave functions of the quasiparticles overlap. As a result of the spatial separation of charge carriers, the recombination probability of electron–hole pairs decreases, which increases the efficiency of charge extraction in photovoltaic devices into the external circuit.

Due to charge separation, the type-II core/shell QDs can have new optical properties that are unavailable in other QDs. Therefore, such nanosystems are intensively studied for the possibility of use in new nanodevices.

Many theoretical and experimental works performed in recent years relate to the study of the optical properties of type-II QDs for use in biomedical and photovoltaic devices (Naifar et al. 2017; Klenovský et al. 2017; Saravanamoorthy and John Peter 2017; Cheche et al. 2013).

Koc and Sahin (2014) and Koç and Sahin (2019) investigated in detail the electronic and optical properties (i.e., binding energy, absorption wavelength, the overlap of electron and hole wave functions, and recombination oscillator strength) of exciton and biexciton in core/shell CdTe/ CdSe-II quantum dot heterostructures.

Tyrrell and Smith (2011) investigated core–shell CdTe/CdSe and CdSe/CdTe type-II quantum dots using the effective mass approximation within single-band and multi-band models. They showed that some of the quantum transitions, which are forbidden in the single-band model, become allowed when considering *s–d* mixing in the valence band.

The influence of the electric field on the electronic states in spherical quantum dots of type-II ZnTe/CdSe was investigated by the variational method in the papers Chafai et al. (2017) and Chafai et al. (2018). Holovatsky et al. (2022) using a simple one-band model within the effective mass approximation, described the effect of an electric field on the energy structure and interband quantum transitions of electrons in spherical quantum dots of type-II CdSe/ZnTe and ZnTe/CdSe. Due to the violation of spherical symmetry by the external electric field, the oscillator strength of quantum transitions forbidden for spherically symmetric systems increases with increasing electric field intensity.

The influence of the magnetic field on the optical properties of multilayer quantum dots has been studied in many papers (Nasri and Bettahar 2016; Çakır et al. 2016; Feddi et al. 2017; Holovatsky et al. 2016, 2017, 2018; Chubrei et al. 2021; Ji et al. 2018; Llorens et al. 2019). These studies show that under the influence of a magnetic field, as a result of a violation of spherical symmetry, the energy levels of quasiparticles are split. At the same time, the role of the ground state of an electron localized in a spherical shell is alternately played by states with a negative value of the magnetic quantum number. This effect of stepwise replacement of the ground state of a quasiparticle with increasing magnetic field in ring-like nanostructures is called the Aharonov–Bohm (A–B) effect. The A–B oscillation was observed using the far-infrared capacitance spectroscopy for self-assembled quantum rings (Fuhrer et al. 2001; Lorke et al. 2000; Yao et al. 2017).

Similar spectral oscillation is expected to appear in the recombination energy of an electron and a hole. But for this, spatial separation of electrons and holes is necessary; otherwise, the total exciton charge is zero, and the A–B effect will not be observed.

In multilayer quantum dots, which consist of two potential wells, the spatial separation of electrons and holes can be achieved due to the localization of quasiparticles in different potential wells that are separated by a barrier. But due to the very small overlap of the wave functions of electrons and holes, it is difficult to observe A–B oscillations for interband absorption.

In type-II quantum dots, the spatial separation of charges is provided by the different positions of wells for electrons and holes, which are not separated by a potential barrier, and therefore, the overlap of wave functions is bigger than for quasiparticles localized in different potential wells in multilayered type-I quantum dots.

For the stacked type-II quantum dots A–B effect was investigated by Sellers et al. (2008a, b) and Kuskovsky et al. (2007, 2017). The authors confirm that excitons in vertically stacked quantum dots of type-II demonstrate A–B oscillations in radiation intensity when the magnetic field increases.

Studies of the A–B effect in spherical core–shell type-II QDs have not yet been performed. The present investigation aims to determine the magnetic field impact on the energy structure and interband optical quantum transitions in type-II spherical quantum dots. For this purpose, the dependencies of the energy spectra and wave functions of an electron and hole on the magnetic field induction

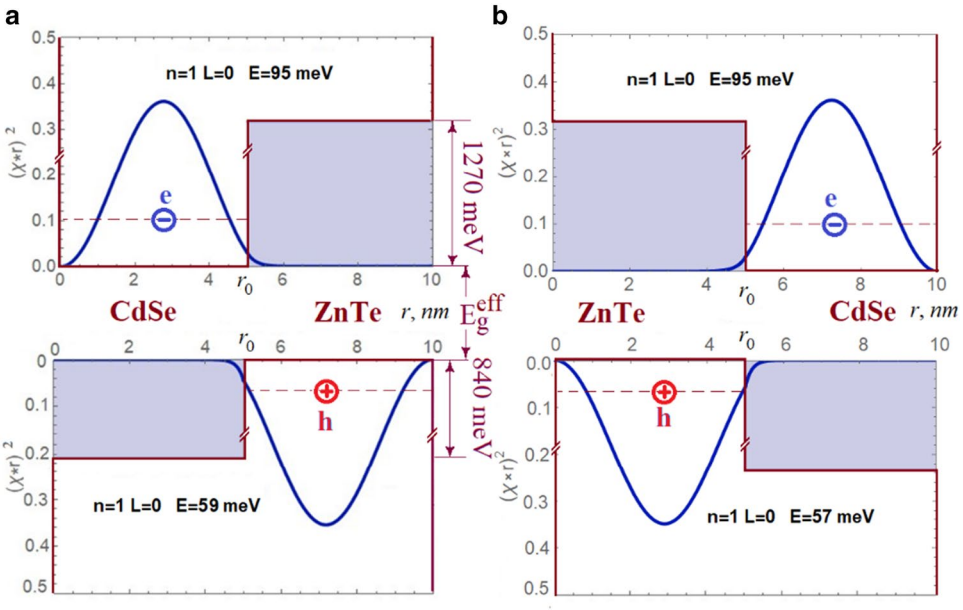

Fig. 1 The scheme potential energies of electron and hole in QDs type-II CdSe/ZnTe and ZnTe/CdSe

are calculated by the diagonalization method for spherical quantum dots ZnTe/CdSe and CdSe/ZnTe with different sizes of core.

This paper presents a study of the effect of a magnetic field on the energy spectrum of a ZnTe/CdSe type-II spherical quantum dot, in which the electron is localized in the shell, and its energy spectrum has A–B oscillations. The same oscillations occur for the hole ground state in the inverse quantum dot (CdSe/ZnTe).

The organization of the paper is as follows: Sect. 1 contains the theoretical framework, in Sect. 2, we discussed the obtained results, and in Sect. 3, we report our conclusions.

Theoretical framework

The spherical semiconductor QDs type-II ZnTe/CdSe and reversed CdSe/ZnTe are under study. In order to investigate the effect of magnetic field on the electron and hole energy spectrum and wave functions, the Schrodinger equation is solved

The Schrödinger equations for the confined electron (hole) in core–shell QD under external magnetic are given by

$$H_{e(h)}\Psi_{\mathrm{jm}}^{e(h)}\left(\vec{r}\right) = E_{\mathrm{jm}}^{e(h)}\ \Psi_{\mathrm{jm}}^{e(h)}(\vec{r}), \tag{1}$$

are to be solved. The Hamiltonian $H_{e(h)}$ has the form

$$H_{e(h)} = \left(\vec{p} - \frac{e}{c}\vec{A}\right)\frac{1}{2\,\mu_{e(h)}(r)}\left(\vec{p} - \frac{e}{c}\vec{A}\right) + U_{e(h)}(r), \tag{2}$$

where $\vec{A}$is the vector potential, confining potential $U_{e(h)}(r)$ and effective mass $\mu_{e(h)}(r)$ for DQ CdSe/ZnTe has form

$$U_e(r) = \begin{cases} 0, & r \le r_0 \\ V_e, & r_0 < r \le r_1 \\ \infty, & r > r_1 \end{cases},$$
$$U_h(r) = \begin{cases} V_h, & r \le r_0 \\ 0, & r_0 < r \le r_1 \\ \infty, & r > r_1 \end{cases}, \tag{3}$$

$$\mu_{e(h)}(r) = \begin{cases} m_0^{e(h)}, & r \le r_0 \\ m_1^{e(h)}, & r_0 < r \le r_1 \end{cases}. \tag{4}$$

For QD ZnTe/CdSe in formula (3), it is necessary to replace the indices e and h.

Taking into account the relationship between vector potential $\vec{A}$ and magnetic field induction $\vec{B}$: $\vec{A} = [\vec{r} \times \vec{B}]/2$, the Hamiltonian (2) is rewritten as

$$H_{e(h)} = -\frac{\hbar^2}{2}\vec{\nabla}\frac{1}{\mu_{e(h)}(r)}\vec{\nabla} + \frac{\mathrm{eB}}{2c\mu_{e(h)}(r)}L_z + \frac{e^2B^2r^2\sin^2\theta}{8c^2\mu_{e(h)}(r)} + U_{e(h)}(r). \tag{5}$$

In order to solve Eq. (1), the wave functions are expanded over the complete set of the exact solutions of the Schrödinger equation for an electron in the same QD without the magnetic fields

$$\Psi_{\mathrm{jm}}^{e(h)}(\vec{r}) = \sum_n \sum_l c_{\mathrm{jnlm}}^{e(h)}\Phi_{\mathrm{nlm}}^{e(h)}(\vec{r}). \tag{6}$$

Due to the spherical symmetry of the problem, the wave function of the electron will take the form

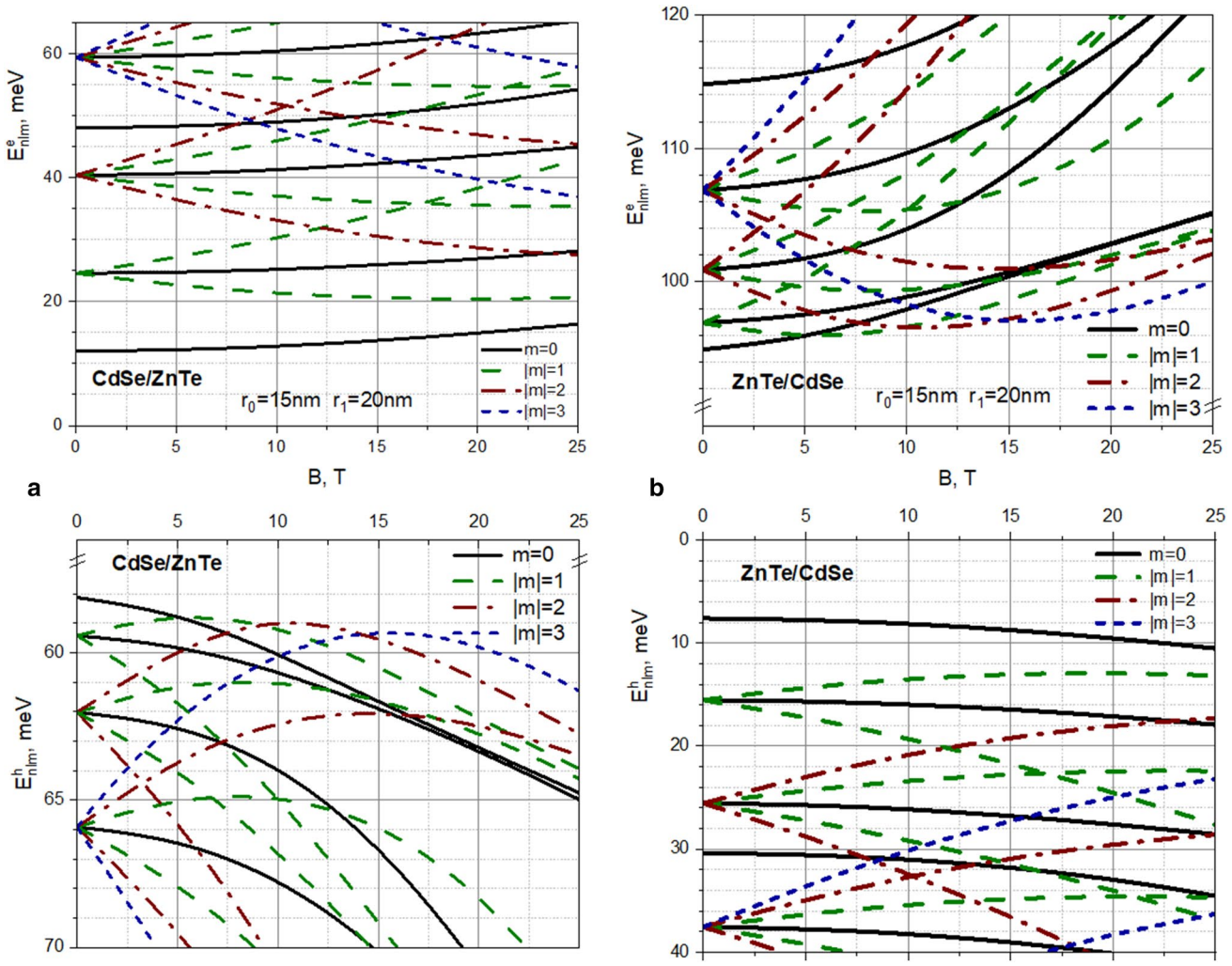

Fig. 2 Electron and hole energies in QD CdSe/ZnTe (a) and ZnTe/CdSe (b) as a function of the magnetic field induction B ($r_0 = 15$ nm, $r_1 - r_0 = 5$ nm)

$\Phi^{e(h)}_{\text{nlm}}(\vec{r}) = R^{e(h)}_{\text{nl}}(r)Y_{\text{lm}}(\theta,\phi)$, where $Y_{lm}(\theta,\phi)$—spherical functions, the radial parts $R^{e(h)}_{\text{nl}}(r)$ are linear combination of Bessel functions of the first and second kind j_l, n_l for QD core and shell. Taking to account the large bandgap of the external medium, we obtain $R^{e(h)(1)}_{\text{nl}}(r_1) = 0$. The electron and hole energy spectra $E^{e(h)}_{\text{nl}}$ are found by using Ben–Daniel–Duke boundary conditions:

$$\left.\begin{array}{c} R^{e,h(0)}_{nl}(r_0) = R^{e,h(1)}_{nl}(r_0) \\ \frac{1}{m_0}\frac{dR^{e,h(0)}_{nl}(r)}{dr}\,|_{r=r_0} = \frac{1}{m_1}\frac{dR^{e,h(1)}_{nl}(r)}{dr}\,|_{r=r_0} \end{array}\right\}. \tag{7}$$

The expansion coefficients $c^{e(h)}_{\text{jnlm}}$ and quasiparticles energy spectra $E^{e(h)}_{\text{jm}}$ are obtained by the diagonalization method. The new functions $\Psi^{e(h)}_{\text{jm}}(\vec{r})$, with the fixed value of the magnetic quantum number, are obtained from the expansion (6), over the wave functions $\Phi^{e(h)}_{\text{nlm}}(\vec{r})$ with the same m. The electron and hole states are characterized by two quantum numbers j and m. Here, j denotes the number of the energy level at fixed m. The interband transition energy is given by

$$E_{e-h} = E^*_g + E^e_i + E^h_j - E^b_{\text{ex}}, \tag{8}$$

where $E^*_g = E^{\text{CdSe}}_g - V_h = E^{\text{ZnTe}}_g - V_e$ is the effective energy gap between the bottom CdSe conducting band and top ZnTe valence band (Fig. 1), E^b_{ex} – the electron and hole Coulomb interaction energy. The Coulomb term is calculated in the first order of perturbation theory (Wu and Cheng 2018; Holovatsky et al. 2022):

$$E^b_{ex} = \frac{2}{\varepsilon}\iint \frac{|\,\Psi^{ex}_{if}(\vec{r}_e,\vec{r}_h)\,|^2}{|\,\vec{r}_e - \vec{r}_h\,|}d\vec{r}_e d\vec{r}_h, \tag{9}$$

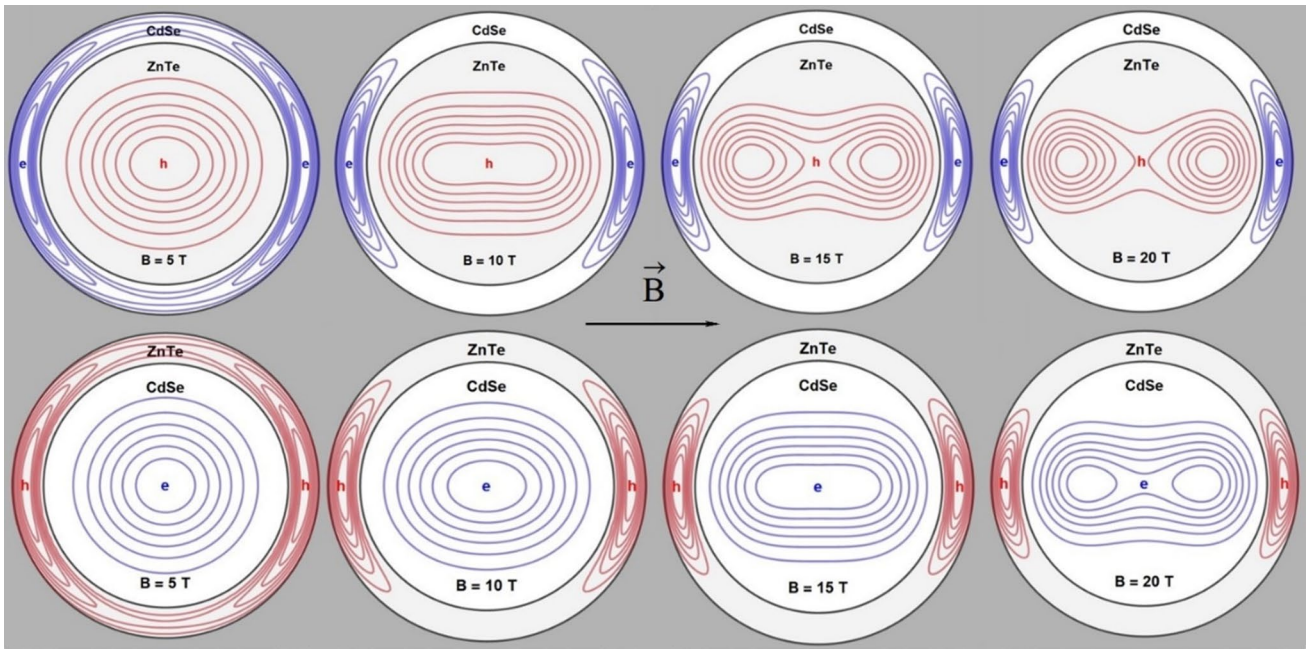

Fig. 3 The evolution of the probability density distribution $|\Psi_{100}(\vec{r})|^2$ for an electron and a hole in the core–shell QD under the influence of a magnetic field (upper row—ZnTe/CdSe, lower row—CdSe/ZnTe)

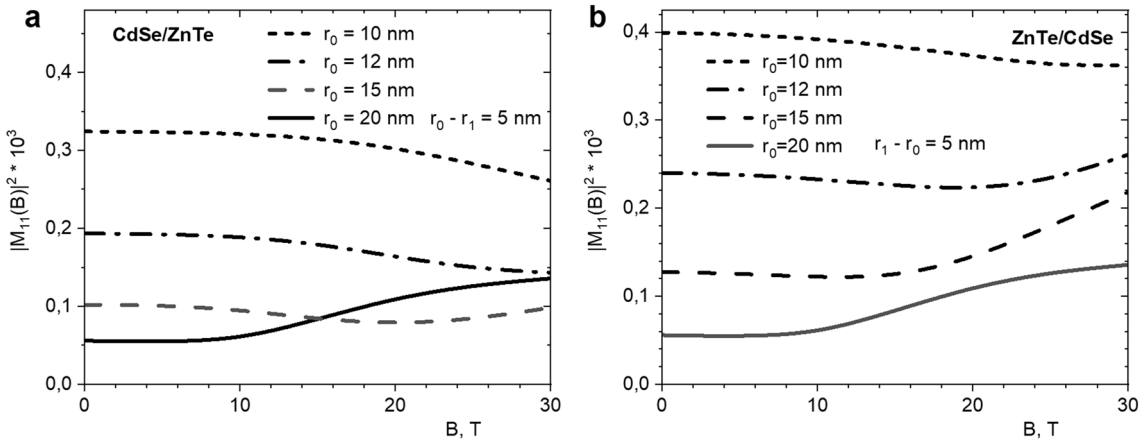

Fig. 4 Dependence $|M_{10,10}|^2$ on the magnetic field for QDs CdSe/ZnTe (a) and ZnTe/CdSe (b) with different core radius ($r_0 = 12, 15, 20$ nm, $r_1 - r_0 = 5$ nm)

where $\Psi_{ij}^{ex}(\vec{r}_e, \vec{r}_h) = \Psi_i^e(\vec{r}_e)\Psi_j^h(\vec{r}_h)$, $\varepsilon = \sqrt{\varepsilon_{\mathrm{CdSe}}\varepsilon_{\mathrm{ZnTe}}}$ – average dielectric constant. The Rydberg and Bohr radius are taken to be the energy and length units, respectively.

Using wave function and energies quantum transition, we also investigate the optical absorption coefficient of QDs. The general form of the exciton absorption coefficient of a single QD is given by Sahin et al. (2009)

$$\alpha(\hbar\omega) \propto \sum_k f_k \delta_k(\hbar\omega - E_{e-h}) \tag{10}$$

The oscillator strength of the interband quantum transitions defines the strength of absorption lines can be obtained (Wu and Cheng 2018; Cheche et al. 2013) as

$$f_{ij} = \frac{E_p}{2E_{e-h}}|M|_{ij}^2, \tag{11}$$

where $M_{ij} = \int_V \Psi_i^{e*}(\vec{r})\Psi_j^h(\vec{r})d\vec{r}$ – matrix element of the interband transition, E_p – Kane energy, which is 21 eV for CdSe (Sahin et al. 2009) and 19.1 eV for ZnTe (Cheche et al. 2013).

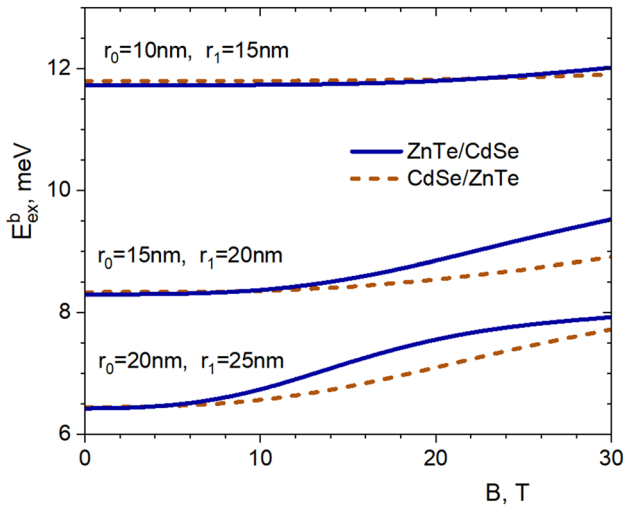

Fig. 5 Dependence $E_{ex}^{b}(B)$ for QD ZnTe/CdSe (solid lines) and CdSe/ZnTe (dashed lines) with different core radius ($r_0 = 10, 12, 15nm, r_1 - r_0 = 5nm$)

Results and discussion

The computer calculations were performed for CdSe/ZnTe and ZnTe/CdSe nanostructure with the following physical parameters (Chafai et al. 2017):

$$\text{CdSe:} m_e = 0.13, m_h = 0.45,\ E_g = 1.75\ \text{eV},\ \varepsilon_{CdSe} = 10.6;$$
$$\text{ZnTe:}\ m_e = 0.15, m_h = 0.2, E_g = 2.2\text{eV}, \varepsilon_{ZnTe} = 9.7;$$
$$r_0 = 10 \div 20\text{nm}, r_1 - r_0 = 5\text{nm}, V_e = 1270\text{meV}, V_h = 840\ \text{meV}.$$

For calculating the influence of magnetic field, we took into account not less than 20 terms in the expansion (6).

In Fig. 2, the dependencies of the electron and hole energies in QDs CdSe/ZnTe and ZnTe/CdSe on the magnetic field induction are shown.

The figure proves the orbital $(2l + 1)$-fold degeneracy is removed when a magnetic field is applied. This happens due to the splitting of the applied magnetic field. For example, the first excited state m can take three values 1, 0, and –1. In addition, the energy of quasiparticle states with m>0 increases monotonically with the increasing magnetic field, while for states with m<0, the non-monotonic dependence of energy on the magnetic field is due to the linear and quadratic terms for the magnetic field in the Hamiltonian (5). It is clearly visible that for quasiparticles localized in the shell, the rate of energy decay is greater at large values of $|m|$, which leads to the crossing of all lower energy levels and therefore the ground state is formed from states with different magnetic numbers.

Figure 3 shows the evolution of the probability density distribution $|\Psi_{10}(\vec{r})|^2$ for an electron and a hole in the core–shell QD with $r_0 = 20$ nm, $r_1 = 25$ nm under the influence of a magnetic field.

The magnetic field deforms the distributions of electron and hole densities in QD. The angular probability increases near $\theta = 0,\ \pi$ and decreases near $\theta = \pi/2$ at the magnetic field induction increases. The wave function 1s state of the quasiparticle, which is localized in the shell is characterized by the most obvious deformation. Its view approaches the form of the excited 1p state under the influence of a magnetic field. Therefore, the energies of the 1$s$and 1p states converge when the magnetic field increases.

The behavior of the wave functions Ψ_{10}^{e} and Ψ_{10}^{h} under the influence of a magnetic field (Fig. 3) is reflected in their overlap on the core–shell interface. Figure 4 shows dependences of $|M_{10,10}|^2$ on the magnetic field for QDs CdSe/ZnTe and ZnTe/CdSe with different core sizes. The dependences of the matrix element square $|M_{10,10}|^2$ on the magnetic field are non-monotonic due to the contribution of various factors: a decrease in the overlap of the wave functions in the direction perpendicular to the induction of the magnetic field and an increase in the overlap in the direction parallel to the magnetic field. The overlap of the wave functions is very small at large sizes of the quantum dot core, but under the influence of a magnetic field due to the deformation of the wave function, the overlap increases.

Figure 5 shows that the electron–hole interaction energy also increases with increasing magnetic field induction. For quantum dots with a larger core radius, the electron–hole interaction energy is lower, but the effect of the magnetic field is greater.

To evaluate the possibility of observing A–B oscillations during interband absorption, consider the dependence of the energies of quantum transitions between different states of an electron and a hole, which are shown in Fig. 6.

Figure 6a and c shows that the quantum transitions with $\Delta m = 0$, which is allowed by the selection rules does not have A–B oscillations. But quantum transitions between the ground state of the quasiparticle localized in the core and the states $m = 0, -1, -2, -3, \ldots$ of the quasiparticle localized in the shell show A–B oscillations (Fig. 6b, d). Although last transitions are forbidden by selection rules in angular momentum, they are strictly valid only for the situation of perfect rotational symmetry and low temperatures. Real QDs always have defects and do not have perfect symmetry, so it is possible to observe A–B oscillations of interband transitions.

The effects we observe in our heterostructure when introducing an external magnetic field are not observable just by changing the non-magnetic semiconductor to a magnetic one. For example, the combination of the core/shell 3D heterostructure and the externally applied magnetic field gives rise to ground state oscillations for the electron or

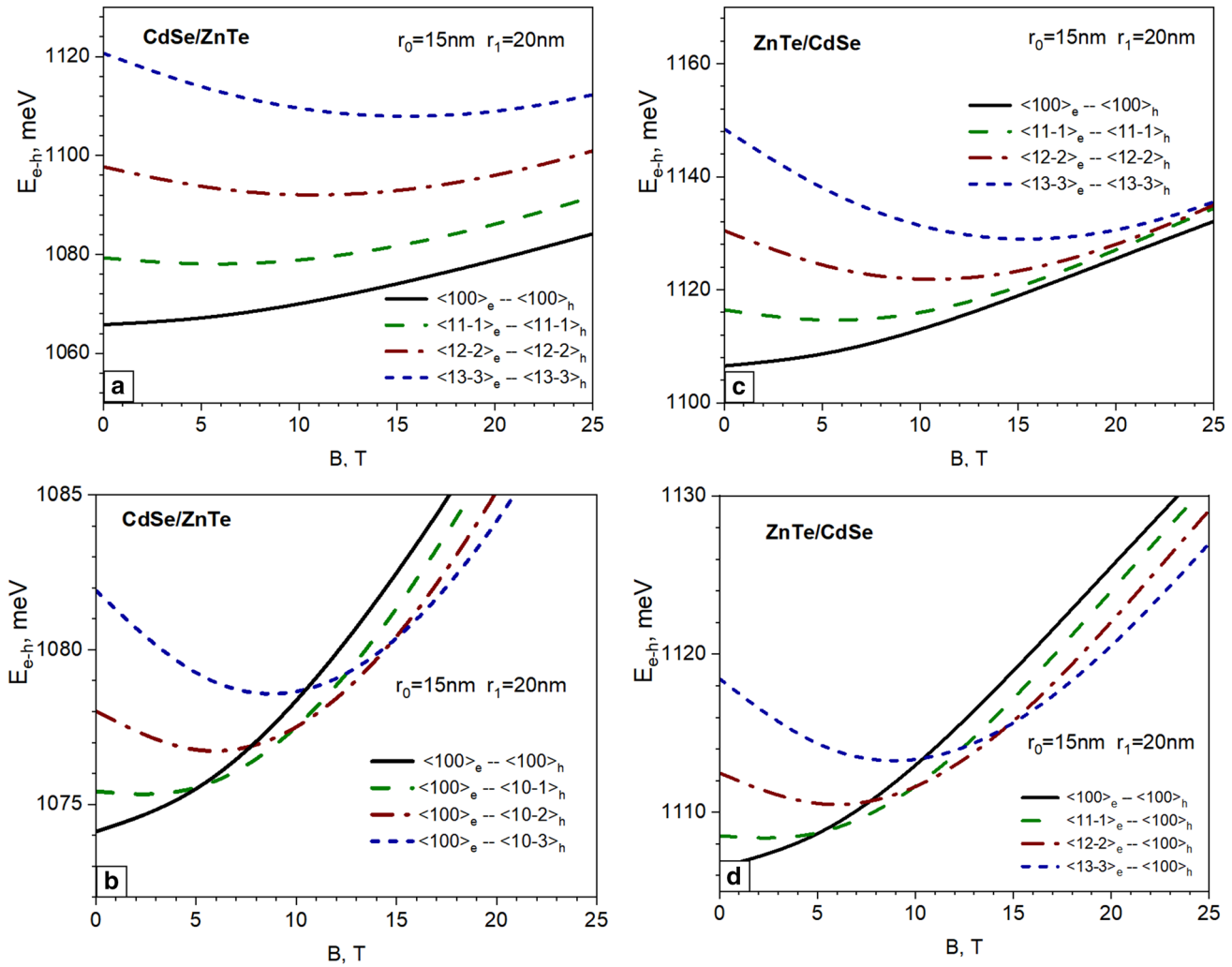

Fig. 6 Dependence interband transition energies $E_{e-h}(B)$ for QDs CdSe/ZnTe (a, b) and ZnTe/CdSe (c, d)

hole, depending on which material is located in the shell region. The presence of the external magnetic field on the 3D spherically symmetric structure breaks the spherical symmetry of the problem, preserving the axial symmetry concerning the plane perpendicular to the applied magnetic field. This would also not be observable just by changing the semiconductor type.

The semiconductors we have used in this manuscript have been the research subject in recent years for different reasons, which we expose here. First, this type of core/shell quantum dots are also known as colloidal quantum dots, which are obtained extremely easily by dripping a semiconductor into a substance that supports it and behaves like an infinite potential barrier. Colloidal quantum dots are being widely used in applications for biophysics, communications, energy emission and reception, and solar cells. These semiconductors are attractive because when forming the core/shell system, the electron and the hole are located in different regions of space. The electron is located in the CdSe region, while the hole is confined to the ZnTe. Therefore, depending on who is the core and who is the shell, we can have oscillations of the ground state as a function of the magnetic field either for the electron, when the core is formed by CdSe, or oscillations of the ground state of the hole when the shell it is formed by ZnTe. These electron and hole systems in different regions of space give rise to the well-known spatially indirect excitonic states. Systems where, due to the reduced overlapping of the electron and hole wave functions, the exciton has a long lifetime. Likewise, this situation gives rise to a small binding energy of the excitonic state. All this corresponds to open issues in the literature that deserve investigation to expand the potential technological applications of these heterostructures.

Conclusion

We have theoretically investigated the effect of the magnetic field on the energy levels in spherical core–shell QDs of the type-II. To find the energy levels and wave functions of the electron and hole, we used the diagonalization method within the effective mass approximation. The overlap of the wave functions and the energy of the Coulomb interaction between an electron and a hole increases with increasing magnetic field induction. The energies of interband quantum transitions permitted by the selection rules do not contain A–B oscillations, while such oscillations are possible for forbidden transitions. Therefore, under real experimental conditions, in the absence of perfect symmetry, absorption lines may appear in the low-energy part of the spectrum, which are formed with the participation of quasiparticle states with different values of the magnetic quantum number. It may be important in the quantitative understanding of future experimental work involving excitons in QDs. The present results are useful in understanding the optical and magnetic properties of core–shell QDs of the type-II.

It is shown that the magnetic field violates the spherical symmetry of the system and takes off the degeneration of the energy spectrum with respect to the magnetic quantum number. The quasiparticle energy in states with $m \geq 0$ monotonously increases when the magnetic field enhances and these dependencies are non-monotonous in states with $m < 0$. The electron ground state energy in ZnTe/CdSe and the hole ground state energy in CdSe/ZnTe are formed alternately by the lowest states $m = 0, -1, -2, \ldots$ with increasing the induction of magnetic field (Aharonov–Bohm effect). The magnetic field affects the overlap of electron and hole wave functions and, therefore, the strength of the quantum transitions oscillator depends on the magnetic field induction. It is shown that the Aharonov–Bohm effect can be observed in the interband quantum transitions.

Data availability The data used to support the findings of this study are available from the corresponding author upon request.

Declarations

Conflict of interest The authors declare that they have no conflict of interest.

References

AbouElhamd AR, Al-Sallal KA, Hassan A (2019) Review of core/shell quantum dots technology integrated into building's glazing. Energies. https://doi.org/10.3390/en12061058

Çakır B, Atav Ü, Yakar Y, Özmen A (2016) Calculation of Zeeman splitting and Zeeman transition energies of spherical quantum dot in uniform magnetic field. Chem Phys 475:61–68. https://doi.org/10.1016/j.chemphys.2016.06.010

Chafai A, Dujardin F, Essaoudi I, Ainane A (2017) Energy spectrum of an exciton in a CdSe/ZnTe type-II core/shell spherical quantum dot. Superlattices Microstruct 101:40–48. https://doi.org/10.1016/j.spmi.2016.11.017

Chafai A, Essaoudi I, Ainane A, Dujardin F, Ahuja R, Chafai A, Essaoudi I, Ainane A (2018) ZnTe/CdSe type-II core/shell spherical quantum dot under an external electric field. Mater Dev 3(1):0504. https://doi.org/10.23647/ca.md20180504

Cheche TO, Barna V, Chang YC (2013) Analytical approach for type-II semiconductor spherical core-shell quantum dots heterostructures with wide band gaps. Superlattices Microstruct 60:475–486. https://doi.org/10.1016/j.spmi.2013.05.027

Chubrei MV, Holovatsky VA, Duque CA (2021) Effect of magnetic field on donor impurity-related photoionisation cross-section in multilayered quantum dot. Philos Mag 101(24):2614–2633

Feddi E, Talbi A, Mora-Ramos ME, El Haouari M, Dujardin F, Duque CA (2017) Linear and nonlinear magneto-optical properties of an off-center single dopant in a spherical core/shell quantum dot. Physica B 524:64–70. https://doi.org/10.1016/j.physb.2017.08.057

Fuhrer A, Lüscher S, Ihn T, Heinzel T, Ensslin K, Wegscheider W, Bichler M (2001) Energy spectra of quantum rings. Nature 413(6858):822–825. https://doi.org/10.1038/35101552

Holovatsky V, Bernik I, Yakhnevych M (2016) Effect of magnetic field on electron spectrum and probabilities of intraband quantum transitions in spherical quantum-dot-quantum-well. Physica E: Low-Dimensional Syst Nanostruct 83:256–262. https://doi.org/10.1016/j.physe.2016.04.035

Holovatsky V, Voitsekhivska O, Yakhnevych M (2017) Effect of magnetic field on an electronic structure and intraband quantum transitions in multishell quantum dots. Physica E 93:295–300. https://doi.org/10.1016/j.physe.2017.06.019

Holovatsky V, Voitsekhivska O, Yakhnevych M (2018) The effect of magnetic field and donor impurity on electron spectrum in spherical core-shell quantum dot. Superlattices Microstruct 116:9–16. https://doi.org/10.1016/j.spmi.2018.02.006

Holovatsky VA, Chubrei MV, Duque CA (2022) Core-shell type-II spherical quantum dot under externally applied electric field. Thin Solid Films. https://doi.org/10.1016/j.tsf.2022.139142

Ji H, Dhomkar S, Wu R, Ludwig J, Lu Z, Smirnov D, Tamargo MC, Bryant GW, Kuskovsky IL (2018) Long spin-flip time and large Zeeman splitting of holes in type-II ZnTe/ZnSe submonolayer quantum dots. J Appl Phys 124(14):144306. https://doi.org/10.1063/1.5041478

Jiao S, Shen Q, Mora-Seró I, Wang J, Pan Z, Zhao K, Kuga Y, Zhong X, Bisquert J (2015) Band engineering in core/shell ZnTe/cdse for photovoltage and efficiency enhancement in exciplex quantum dot sensitized solar cells. ACS Nano 9(1):908–915. https://doi.org/10.1021/nn506638n

Kim S, Kim T, Kang M, Kwak SK, Yoo TW, Park LS, Yang I, Hwang S, Lee JE, Kim SK, Kim SW (2012) Highly luminescent InP/GaP/ZnS nanocrystals and their application to white light-emitting diodes. J Am Chem Soc 134(8):3804–3809. https://doi.org/10.1021/ja210211z

Klenovský P, Steindl P, Geffroy D (2017) Excitonic structure and pumping power dependent emission blue- shift of type-II quantum dots. Sci Rep. https://doi.org/10.1038/srep45568

Koc F, Sahin M (2014) Electronic and optical properties of single excitons and biexcitons in type-II quantum dot nanocrystals. J Appl Phys 115(19):193701. https://doi.org/10.1063/1.4876323

Koç F, Sahin M (2019) The electronic and optical properties of an exciton, biexciton and charged excitons in CdSe/CdTe-based multishell type-II quantum dot nanocrystals. Appl Phys A 125(10):705. https://doi.org/10.1007/s00339-019-3000-3

Kuskovsky IL, MacDonald W, Govorov AO, Mourokh L, Wei X, Tamargo MC, Tadic M, Peeters FM (2007) Optical Aharonov-Bohm

effect in stacked type-II quantum dots. Phys Rev B—Condensed Matter Mater Phys 76(3):1–6. https://doi.org/10.1103/PhysRevB.76.035342

Kuskovsky IL, Mourokh LG, Roy B, Ji H, Dhomkar S, Ludwig J, Smirnov D, Tamargo MC (2017) Decoherence in semiconductor nanostructures with type-II band alignment: all-optical measurements using Aharonov-Bohm excitons. Phys Rev B 95(16):165445. https://doi.org/10.1103/PhysRevB.95.165445

Llorens JM, Oliveira ERCD, Wewiór L (2019) Topology driven g-factor tuning in type-II quantum dots. Phys Rev Appl 10(1):1. https://doi.org/10.1103/PhysRevApplied.11.044011

Long T, Cao J, Jiang ZJ (2019) Predictable spectroscopic properties of type-II ZnTe/CdSe nanocrystals and electron/hole quenching. Phys Chem Chem Phys 21(10):5824–5833. https://doi.org/10.1039/c9cp00026g

Lorke A, Johannes Luyken R, Govorov AO, Kotthaus JP, Garcia JM, Petroff PM (2000) Spectroscopy of nanoscopic semiconductor rings. Phys Rev Lett 84(10):2223–2226. https://doi.org/10.1103/PhysRevLett.84.2223

Ma X, Mews A, Kipp T (2013) Determination of electronic energy levels in type-II CdTe-core/CdSe-shell and CdSe-core/CdTe-shell nanocrystals by cyclic voltammetry and optical spectroscopy. J Phys Chem C 117(32):16698–16708. https://doi.org/10.1021/jp404556b

Naifar A, Zeiri N, Nasrallah SAB, Said M (2017) Optical properties of CdSe/ZnTe type II core shell nanostructures. Optik 146:90–97. https://doi.org/10.1016/j.ijleo.2017.08.079

Nasri D, Bettahar N (2016) Magneto-optical properties in inhomogeneous quantum dot: the Aharonov-Bohm oscillations effect. Physica B 501:68–73. https://doi.org/10.1016/j.physb.2016.08.019

Nizamoglu S, Demir HV (2008) Onion-like (CdSe)ZnS/CdSe/ZnS quantum-dot-quantum-well heteronanocrystals for investigation of multi-color emission. Opt Express 16(6):3515. https://doi.org/10.1364/oe.16.003515

Nizamoglu S, Mutlugun E, Özel T, Demir HV, Sapra S, Gaponik N, Eychmüller A (2008) Dual-color emitting quantum-dot-quantum-well CdSe-ZnS heteronanocrystals hybridized on InGaNGaN light emitting diodes for high-quality white light generation. Appl Phys Lett. https://doi.org/10.1063/1.2898892

Reiss P, Protière M, Li L (2009) Core/shell semiconductor nanocrystals. Small 5(2):154–168. https://doi.org/10.1002/smll.200800841

Sahin M, Nizamoglu S, Kavruk AE, Demir HV (2009) Self-consistent computation of electronic and optical properties of a single exciton in a spherical quantum dot via matrix diagonalization method. J Appl Phys 106(4):0–5. https://doi.org/10.1063/1.3197034

Saravanamoorthy SN, John Peter A (2017) Interband optical transition energies in type-II PbSe/PbS core/shell quantum dots. J Adv Phys 6(1):80–86. https://doi.org/10.1166/jap.2017.1297

Sellers IR, Whiteside VR, Kuskovsky IL, Govorov AO, McCombe BD (2008) Aharonov-Bohm excitons at elevated temperatures in type-II ZnTe/ZnSe quantum dots. Phys Rev Lett 100(13):136405. https://doi.org/10.1103/PhysRevLett.100.136405

Sellers IR, Whiteside VR, Kuskovsky IL, Govorov AO, McCombe BD (2008) Modulation of the Aharonov-Bohm effect in type-II II-V ZnSe: Te quantum dots by a far-infrared laser. Physica E: Low-dimensional Syst Nanostruct 40(6):1819–1823. https://doi.org/10.1016/j.physe.2007.10.049

Selopal GS, Zhao H, Wang ZM, Rosei F (2020) Core/shell quantum dots solar cells. Adv Funct Mater 30(13):1908762. https://doi.org/10.1002/adfm.201908762

Tyagi P, Kambhampati P (2012) Independent control of electron and hole localization in core/barrier/shell nanostructures. J Phys Chem C 116(14):8154–8160. https://doi.org/10.1021/jp212158a

Tyrrell EJ, Smith JM (2011) Effective mass modeling of excitons in type-II quantum dot heterostructures. Phys Rev B—Condensed Matter Mater Phys. https://doi.org/10.1103/PhysRevB.84.165328

Verma S, Kaniyankandy S, Ghosh HN (2013) Charge separation by indirect bandgap transitions in CdS/ZnSe type-II core/shell quantum dots. J Phys Chem C 117(21):10901–10908. https://doi.org/10.1021/jp400014j

Wang L, Nonaka K, Okuhata T, Katayama T, Tamai N (2018) Quasi-Type II Carrier Distribution in CdSe/CdS Core/Shell Quantum Dots with Type i Band Alignment. J Phys Chem C 122(22):12038–12046. https://doi.org/10.1021/acs.jpcc.7b11684

Wu S, Cheng L (2018) Exciton diamagnetic shift and optical properties in CdSe nanocrystal quantum dots in magnetic fields. Physica B: Condensed Matter 534:98–104. https://doi.org/10.1016/j.physb.2018.01.034

Yao Y, Elborg M, Kuroda T, Sakoda K (2017) Excitonic Aharonov-Bohm effect in QD-on-ring nanostructures. J Phys: Condensed Matter 29(38):385301. https://doi.org/10.1088/1361-648X/aa7c90

Zhang W, Chen G, Wang J, Ye BC, Zhong X (2009) Design and synthesis of highly luminescent near-infrared-emitting water-soluble CdTe/CdSe/ZnS Core/Shell/Shell quantum dots Type II. Inorg Chem 48(20):9723–9731. https://doi.org/10.1021/ic9010949

Publisher's Note Springer Nature remains neutral with regard to jurisdictional claims in published maps and institutional affiliations.

Springer Nature or its licensor (e.g. a society or other partner) holds exclusive rights to this article under a publishing agreement with the author(s) or other rightsholder(s); author self-archiving of the accepted manuscript version of this article is solely governed by the terms of such publishing agreement and applicable law.